

The noncentrosymmetric chain compounds, $A_3M_2AsSe_{11}$ ($A = K, Rb, Cs$; $M = Nb, Ta$)

Junghwan Do, Mercuri G. Kanatzidis*

Department of Chemistry, Michigan State University, East Lansing, MI 48824, USA

Received 15 January 2004; received in revised form 1 March 2004; accepted 8 March 2004

Abstract

The noncentrosymmetric niobium and tantalum selenoarsenates, $A_3Nb_2AsSe_{11}$ ($A = K, Rb, Cs$) and $K_3Ta_2AsSe_{11}$, were synthesized in a polyselenoarsenate flux. All compounds crystallize in the polar monoclinic space group Cc . The structures are comprised of the same type of infinite chain anions, $[M_2Se_2(Se_2)_3(AsSe_3)]^{3-}$ ($M = Nb, Ta$) separated by alkali metal cations. The As^{3+} centers with nonbonded electron pairs play an important role in stabilizing the noncentrosymmetric structures. UV-Vis spectroscopy, Raman spectroscopy and differential thermal analysis data are reported. The energy gaps of these compounds vary between 1.35 and 1.53 eV.

© 2004 Elsevier B.V. All rights reserved.

Keywords: Flux synthesis; Non linear optical piezoelectricity; Non-oxide materials

1. Introduction

Recently, we have reported several quaternary tin chalcogenates, $KSnAsS_5$, $K_2SnAs_2S_6$, [1] and $Cs_2SnAs_2Q_9$ ($Q = S, Se$) [2] prepared in polyselenoarsenate fluxes. One important feature that becomes evident in this type of chemistry is that the reactivity of arsenic differs significantly from that of phosphorus. The oxidation of the heavier pnictogen favors predominantly the 3+ state whereas the 4+ and 5+ states are more stable with phosphorus. This divergence lies at the foundation of the bifurcation in chemical reactivity of the two elements and gives rise to the different types of compounds encountered between the chalcophosphate and the chalcogen arsenate phases. The overall symmetry in the structure of the compounds is determined by the arrangement of As^{3+} cations with its lone pair of electrons. In all the cases an antiferroelectric arrangement is found along with a centrosymmetric lattice. Here, we report results of the polyselenoarsenate flux synthesis using early transition metals and describe the niobium/tantalum selenoarsenates, $A_3Nb_2AsSe_{11}$ ($A = K, Rb, Cs$) and $K_3Ta_2AsSe_{11}$. To the best of our knowledge, these compounds are the first quater-

nary alkali metal incorporated group 5 metal chalcogenates. Their structure represents the insertion of As atoms into that of $K_6Nb_4Se_{22}$. All compounds contain infinite chain anions $[M_2AsSe_{11}]^{3-}$ ($M = Nb, Ta$) and adopt the polar space group, Cc which arises from a parallel alignment of the $[AsSe_3]^{3-}$ pyramids.

2. Experimental

2.1. Reagents

The following reagents were used as obtained: Nb (99.9 %; Aldrich Chemical Co, Milwaukee, WI), Ta (99.8 %; Cerac, Milwaukee, WI), As_2Se_3 (99.9 %; Strem Chemicals, Newburyport, MA), As (99.9%; Aldrich Chemical Co, Milwaukee, WI), Se (99.999 %; Noranda Advanced Materials, Quebec, Canada). *N,N*-dimethylformamide (Spectrum Chemicals, ACS reagent grade); diethyl ether. K_2Se , Rb_2Se and Cs_2Se starting materials were prepared by stoichiometric reactions of potassium, rubidium, cesium metal and selenium in liquid NH_3 .

2.2. Synthesis

Compound $K_3Nb_2AsSe_{11}$ (**1**) was synthesized from a mixture of 0.157 g (1.0 mmol) K_2Se , 0.092 g (1.0 mmol)

* Corresponding author. Tel.: +1-517-355-9715-174; fax: +1-517-353-1793.

E-mail address: kanatzid@cem.msu.edu (M.G. Kanatzidis).

Nb, 0.193 g (0.5 mmol) As_2Se_3 , and 0.396 g (5.0 mmol) Se. The reagents were mixed, sealed in an evacuated silica tube, and heated at 550 °C for 3 days, then cooled at a rate of 5 °C/h to 250 °C followed by rapid cooling to room temperature. The solid products were washed with *N,N*-dimethylformamide (DMF) to remove the flux and dried with ether. Black rod-shaped single crystals of $\text{K}_3\text{Nb}_2\text{AsSe}_{11}$ were obtained together with big black polyhedra, Nb_2Se_9 as indicated by X-ray powder diffraction and energy dispersive spectroscopy (EDS). Quantitative synthesis of pure $\text{K}_3\text{Nb}_2\text{AsSe}_{11}$ was achieved by a reaction of stoichiometric amounts of $\text{K}_2\text{Se}/\text{Nb}/\text{As}/\text{Se}$ at 550 °C. The product was stable in air and water. EDS analysis of a number of crystals gave an average nominal formula of “ $\text{K}_3\text{Nb}_2\text{AsSe}_{11}$ ”. The errors in these analyses are to within $\pm 4\%$.

$\text{Rb}_3\text{Nb}_2\text{AsSe}_{11}$ (**2**) was synthesized from a mixture of 0.250 g (1.0 mmol) Rb_2Se , 0.092 g (1.0 mmol) Nb, 0.193 g (0.5 mmol) As_2Se_3 , and 0.396 g (5.0 mmol) Se. The reagents were mixed, sealed in an evacuated silica tube, and heated at 550 °C for 3 days, then cooled at a rate of 5–250 °C/h followed by rapid cooling to room temperature. The solid products were washed with DMF to remove the flux and dried with ether. Black rod-shaped single crystals of $\text{Rb}_3\text{Nb}_2\text{AsSe}_{11}$ were obtained in pure form (yield 92% based Nb). Quantitative synthesis of pure $\text{Rb}_3\text{Nb}_2\text{AsSe}_{11}$ was also achieved by a reaction of the stoichiometric amounts of $\text{Rb}_2\text{Se}/\text{Nb}/\text{As}/\text{Se}$ at 550 °C. The product was stable in air and water in the order of several days. EDS analysis of the crystals gave a nominal formula of “ $\text{Rb}_3\text{Nb}_2\text{AsSe}_{11}$ ”.

$\text{Cs}_3\text{Nb}_2\text{AsSe}_{11}$ (**3**) was synthesized from a mixture of 0.345 g (1.0 mmol) Cs_2Se , 0.092 g (1.0 mmol) Nb, 0.193 g (0.5 mmol) As_2Se_3 , and 0.396 g (5.0 mmol) Se. The reagents were mixed, sealed in an evacuated silica tube, and heated at 550 °C for 3 days, then cooled at a rate of 5–250 °C/h followed by rapid cooling to room temperature. The solid products were washed with DMF) and ether. Pure black rod-shaped single crystals of $\text{Cs}_3\text{Nb}_2\text{AsSe}_{11}$ were obtained (yield 94% based on Nb). The product was stable in air and water for several days. EDS analysis of the crystals gave an average nominal formula of “ $\text{Cs}_3\text{Nb}_2\text{AsSe}_{11}$ ”.

$\text{K}_3\text{Ta}_2\text{AsSe}_{11}$ (**4**) was synthesized from a mixture of 0.158 g (1.0 mmol) K_2Se , 0.181 g (1.0 mmol) Ta, 0.193 g (0.5 mmol) As_2Se_3 , and 0.317 g (4.0 mmol) Se. The reagents were mixed, sealed in an evacuated silica tube, and heated at 550 °C for 3 days, then cooled at a rate of 5–250 °C/h followed by rapid cooling to room temperature. The solid products were washed with DMF and ether. Isolation produced a single phase of pure black rod-shaped single crystals of $\text{K}_3\text{Ta}_2\text{AsSe}_{11}$ (yield 88% based on Ta). The product was stable in air and water. Quantitative synthesis of pure $\text{K}_3\text{Ta}_2\text{AsSe}_{11}$ was also achieved by a reaction of stoichiometric amounts of $\text{K}_2\text{Se}/\text{Ta}/\text{As}/\text{Se}$ at 550 °C. The product was stable in air and water. EDS analysis of the crystals gave “ $\text{K}_3\text{Ta}_2\text{AsSe}_{11}$ ”. The structural details of the compounds were determined by a single-crystal X-ray diffraction study.

All compounds **1–4** are insoluble in polar solvents, such as DMF and dimethylsulfoxide.

3. Physical characterization techniques

3.1. X-ray powder diffraction

Analyses were performed using a calibrated CPS 120 INEL X-ray powder diffractometer (Cu $\text{K}\alpha$ radiation) operating at 40 kV/20 mA and equipped with a position-sensitive detector with a flat sample geometry.

3.2. Electron microscopy

Semi quantitative analyses of the compounds were performed with a JEOL JSM-35C scanning electron microscope (SEM) equipped with a Tracor Northern energy dispersive spectroscopy (EDS) detector.

3.3. Solid state UV-Vis

Optical diffuse reflectance measurements were performed at room temperature using a Shimadzu UV-3101 PC double-beam, double-monochromator spectrophotometer operating in the 200–2500 nm region. The bands gaps were derived using a protocol reported elsewhere [3].

3.4. Raman spectroscopy

Raman spectra were recorded on a Holoprobe Raman spectrograph equipped with a CCD camera detector using 633 nm radiation from a HeNe laser for excitation and a resolution of 4 cm^{-1} . Laser power at the sample was estimated to be about 5 mW and the focused laser beam diameter was ca. 10 μm . Sixty-four scans were sufficient to obtain good quality spectra.

3.5. Differential thermal analysis (DTA)

DTA experiments were performed on Shimadzu DTA-50 thermal analyzer. Typically a sample (~20 mg) of ground crystalline material was sealed in a silica ampoule under vacuum. A similar ampoule of equal mass filled with Al_2O_3 was sealed and placed on the reference side of the detector. Sample **1** was heated to 650 °C at 10 °C/min, and after 3 min it was cooled at a rate of $-10\text{ °C}/\text{min}$ to 50 °C. A sample of **2** was heated to 600 °C using the same cycle as above. Residues of the DTA experiments were examined by X-ray powder diffraction. Reproducibility of the results was checked by running multiple heating/cooling cycles.

3.6. X-ray crystallography

The crystal structures of **1–4** were determined by single-crystal X-ray diffraction methods. Preliminary

Table 1
Crystallographic details for 1–4

Empirical formula	K ₃ Nb ₂ AsSe ₁₁ (1)	Rb ₃ Nb ₂ AsSe ₁₁ (2)	Cs ₃ Nb ₂ AsSe ₁₁ (3)	K ₃ Ta ₂ AsSe ₁₁ (4)
fw	1246.60	1385.71	1528.03	1422.68
Space group	<i>Cc</i>	<i>Cc</i>	<i>Cc</i>	<i>Cc</i>
<i>a</i> (Å)	14.944(6)	15.111(2)	15.254(3)	14.924(3)
<i>b</i> (Å)	12.916(5)	13.242(2)	13.748(3)	12.938(2)
<i>c</i> (Å)	9.945(4)	10.041(2)	10.187(2)	9.943(2)
β (°)	100.483(6)	99.768(2)	98.367(4)	100.319(3)
<i>V</i> (Å ³)	1887.6(13)	1980.2(5)	2113.6(8)	1888.9(5)
<i>Z</i>	4	4	4	4
Crystal size (mm ³)	0.12 × 0.13 × 0.34	0.09 × 0.12 × 0.30	0.11 × 0.14 × 0.40	0.10 × 0.12 × 0.42
ρ_{calcd} (g/cm ³)	4.387	4.648	4.802	5.003
μ (cm ⁻¹)	248.02	303.38	266.52	351.49
<i>T</i> (K)	296(2)	296(2)	296(2)	296(2)
λ (Å)	0.71073	0.71073	0.71073	0.71073
θ range (°)	2.10–28.25	2.06–28.29	2.00–28.44	2.10 to 28.30
Absolute structure parameter	0.050(8)	0.03(1)	0.05(1)	0.22(1)
R1 [<i>I</i> > 2 σ (<i>I</i>)] ^a	0.0281	0.0392	0.0298	0.0226
wR2 (all data) ^b	0.0697	0.1028	0.0712	0.0570

^a $R_w = \sum ||F_0| - |F_c|| / \sum |F_0|$.

^b $wR2 = \{ \sum [w(F_0^2 - F_c^2)^2] / \sum [w(F_0^2)^2] \}^{1/2}$.

examination and data collection were performed on a SMART platform diffractometer equipped with a 1 K CCD area detector using graphite monochromatized Mo K α radiation at room temperature. A hemisphere of data was collected with narrow scan widths of 0.30° in ω and an exposure time of 30 s per frame for 1–4. The data were integrated using the SAINT program [3]. For 1–4 the program SADABS was used for the absorption correction. Additional crystallographic data for 1–4 are given in Table 1. In all cases satisfactory refinements were obtained with the noncentrosymmetric space group, *Cc*.

The initial positions for all atoms were obtained with direct methods and the structures were refined with full-matrix least-squares techniques using SHELXTL [4]. The *R* values for the final cycle of the refinements based on F_0^2 are given in Table 1. Final values of selected bond lengths and angles are given in Table 2.

4. Results and discussion

4.1. Synthesis

All the compounds 1–4 were prepared by using a flux ratio of 2:2:1:10 A₂Se/Nb/As₂Se₃/Se (A = K, Rb, Cs) at 550 °C. The influence of flux basicity on the reaction outcome was explored in some detail in order to better appreciate its role in phase formation in this system. Such a flux basicity investigation should always be performed where possible.

A change in the flux basicity was achieved by altering the A₂Se:Se (A = K, Rb, Cs) ratio from 1:10 to 4:10. In the case of potassium, increasing this ratio to 3:10, gives the phase of 1 forms without Nb₂Se₉, but mixed with the water soluble K₃AsSe₄. Increasing the A₂Se:Se ratio to 4:10, the phase of 1 no longer forms; instead, the system

phase-separates to produce K₁₂Nb₆Se₃₅, (EDS analysis and single crystal X-ray diffraction analysis confirmed it to be isostructural to Rb₁₂Nb₆Se₃₅) [5] and K₃AsSe₄. Decreasing the ratio to 1:10 led to pure Nb₂Se₉. In the case of rubidium, increasing the ratio to 3:10 and 4:10 led to the formation of 2 along with Rb₃AsSe₄. Decreasing the ratio to 1:10 again produced exclusively Nb₂Se₉. In the Cs system, increasing the ratio to 3:10 formed the phase of 3 together with black rods. Electron microscope analysis of the black rod crystals gave an average composition of Cs_{2.9}Nb₂Se_{11.3} and upon single crystal X-ray diffraction analysis proved to be Cs₃Nb₂Se₁₁, which is isostructural to K₃Nb₂Se₁₁ [6] More basic conditions (4:10) produced 3 together with Cs₃NbSe₄ and Cs₂₁(Nb₄Se₂₂)₃(AsSe₃) containing isolated [Nb₄Se₂₂]⁶⁻ and [AsSe₃]³⁻ anions. [7] In the less basic flux (1:10), again single phase Nb₂Se₉ was observed. It is apparent in all systems that increased fractions of A₂Se (more basic) favor the formation of Nb⁵⁺ containing species such as [Nb₂Se₁₁]³⁻ and [NbSe₄]³⁻ as found in K₁₂Nb₆Se₃₅, Cs₃Nb₂Se₁₁, and Cs₃NbSe₄, whereas reactions with lower A₂Se content (less basic) give Nb⁴⁺ compounds such as Nb₂Se₉: 2Nb⁴⁺2(Se₂)²⁻(Se₅)²⁻.

4.2. Structures

The crystal structure type of A₃Nb₂AsSe₁₁ (A = K, Rb, Cs) 1–3 is polar and adopts the space group *Cc*. The structure of 1–3 is composed of chain anions 1/ ∞ [Nb₂AsSe₁₁]³⁻ separated by alkali metal cations, Fig. 1. Each of the two crystallographically independent niobium atoms in the chain is coordinated by seven selenium atoms in a distorted pentagonal bipyramidal arrangement. Two pentagonal prisms one containing a Nb⁵⁺ ion coordinated by 3Se²⁻ and 3Se₂²⁻ ligands and the other containing a Nb⁵⁺ ion coordinated by 2Se²⁻ and 3Se₂²⁻ ligands share

Table 2
Bond lengths (Å) and angles (°) for **1–4**

For 1			
K(1)-Se(9)#1	3.266(3)	K(1)-Se(11)	3.269(3)
K(1)-Se(10)#2	3.345(3)	K(1)-As#3	3.451(3)
K(1)-Se(11)#1	3.530(3)	K(1)-Se(2)	3.604(3)
K(1)-Se(5)	3.722(3)	K(1)-Se(5)#4	3.737(3)
K(1)-Se(1)#4	3.896(3)	K(1)-Se(7)#4	3.918(3)
K(1)-Se(1)	3.935(3)		
K(2)-Se(8)	3.311(2)	K(2)-Se(11)#5	3.355(3)
K(2)-Se(6)#6	3.396(3)	K(2)-Se(9)#7	3.426(3)
K(2)-Se(3)#7	3.443(2)	K(2)-Se(11)#6	3.491(3)
K(2)-Se(1)#6	3.503(2)	K(2)-Se(10)	3.538(3)
K(2)-Se(10)#7	3.672(3)	K(2)-Se(7)	3.904(3)
K(3)-Se(4)#8	3.368(3)	K(3)-Se(4)#7	3.466(3)
K(3)-Se(10)#9	3.499(3)	K(3)-Se(8)	3.510(3)
K(3)-Se(6)	3.601(3)	K(3)-Se(3)#7	3.618(3)
K(3)-Se(5)#9	3.677(3)	K(3)-As#7	3.863(3)
K(3)-Se(6)#7	3.905(3)	K(3)-Se(1)	3.915(3)
Nb(1)-Se(10)	2.3244(13)	Nb(1)-Se(8)	2.5936(13)
Nb(1)-Se(3)	2.5979(11)	Nb(1)-Se(7)	2.6444(14)
Nb(1)-Se(5)	2.6939(14)	Nb(1)-Se(2)	2.7490(13)
Nb(1)-Se(1)	2.9269(14)		
Nb(2)-Se(11)	2.3350(13)	Nb(2)-Se(6)	2.5937(12)
Nb(2)-Se(1)	2.6149(14)	Nb(2)-Se(9)	2.6252(13)
Nb(2)-Se(4)	2.6451(12)	Nb(2)-Se(2)	2.6655(14)
Nb(2)-Se(3)	2.8688(13)		
As-Se(4)	2.3780(15)	As-Se(7)#10	2.3796(15)
As-Se(5)#10	2.4338(14)		
Se(1)-Se(6)	2.3714(13)	Se(2)-Se(9)	2.3602(13)
Se(3)-Se(8)	2.3315(13)		
For 2			
Rb(1)-Se(8)#1	3.4082(16)	Rb(1)-Se(11)#2	3.4293(18)
Nb(1)-Se(3)vvRb(1)-Se(6)	3.4852(18)	Rb(1)-Se(9)#3	3.4905(18)
Rb(1)-Se(3)#3	3.5552(16)	Rb(1)-Se(11)	3.5706(18)
Nb(1)-Se(3)	3.5736(16)	Rb(1)-Se(10)#1	3.5803(17)
Rb(1)-Se(10)#3	3.6627(18)	Rb(1)-Se(7)#1	3.9305(19)
Rb(2)-Se(4)#4	3.4448(17)	Rb(2)-Se(8)	3.5752(18)
Rb(2)-Se(4)#5	3.584(2)	Rb(2)-Se(10)#3	3.6276(19)
Rb(2)-Se(6)	3.6575(18)	Rb(2)-Se(3)#5	3.6997(18)
Rb(2)-Se(5)#3	3.7288(19)	Rb(2)-As#5	3.930(2)
Rb(2)-Se(2)#3	3.9484(19)	Rb(2)-Se(6)#5	3.978(2)
Rb(2)-Se(1)	3.989(2)		
Rb(3)-Se(11)#6	3.3296(19)	Rb(3)-Se(9)	3.3572(17)
Rb(3)-Se(10)#7	3.4729(19)	Rb(3)-As#8	3.5358(19)
Rb(3)-Se(11)	3.6013(19)	Rb(3)-Se(2)#6	3.7327(18)
Rb(3)-Se(5)#9	3.7528(19)	Rb(3)-Se(5)#6	3.820(2)
Rb(3)-Se(1)#9	3.9672(19)	Rb(3)-Se(7)#9	4.028(2)
Rb(3)-Se(1)#6	4.081(2)		
Nb(1)-Se(10)	2.3293(15)	Nb(1)-Se(8)	2.5949(15)
Nb(1)-Se(3)	2.5985(13)	Nb(1)-Se(7)	2.6507(14)
Nb(1)-Se(5)	2.6994(15)	Nb(1)-Se(2)	2.7500(14)
Nb(1)-Se(1)	2.9347(14)		
Nb(2)-Se(11)	2.3312(15)	Nb(2)-Se(6)	2.5923(14)
Nb(2)-Se(1)	2.6209(14)	Nb(2)-Se(9)	2.6253(15)
Nb(2)-Se(4)	2.6374(14)	Nb(2)-Se(2)	2.6659(15)
Nb(2)-Se(3)	2.8788(14)		
As-Se(4)	2.3767(18)	As-Se(7)#7	2.3816(18)
As-Se(5)#7	2.4300(17)		
Se(1)-Se(6)	2.3719(16)	Se(2)-Se(9)	2.3587(16)
Se(3)-Se(8)	2.3321(14)		

Table 2 (Continued)

For 3			
Cs(1)-Se(8)	3.5234(12)	Cs(1)-Se(11)#1	3.5570(13)
Cs(1)-Se(9)	3.5871(13)	Cs(1)-Se(6)	3.6189(13)
Cs(1)-Se(11)	3.6594(15)	Cs(1)-Se(10)#2	3.6628(13)
Cs(1)-Se(1)	3.6655(12)	Cs(1)-Se(3)	3.7028(12)
Cs(1)-Se(10)	3.7078(14)	Cs(1)-Se(7)#1	4.0262(14)
Cs(1)-Se(7)	4.2375(14)		
Cs(2)-Se(4)#1	3.5479(14)	Cs(2)-Se(8)#3	3.6833(13)
Cs(2)-Se(6)#4	3.7343(14)	Cs(2)-Se(4)	3.7410(15)
Cs(2)-Se(3)#3	3.7945(13)	Cs(2)-Se(10)#4	3.8080(14)
Cs(2)-Se(5)	3.8313(14)	Cs(2)-Se(2)#4	3.9919(14)
Cs(2)-Se(1)#4	4.0773(14)	Cs(2)-As	4.0807(14)
Cs(2)-Se(6)#5	4.0841(15)	Cs(2)-Se(8)#6	4.2566(13)
Cs(3)-Se(11)#1	3.4384(14)	Cs(3)-Se(9)#5	3.4758(13)
Cs(3)-As	3.6253(14)	Cs(3)-Se(10)	3.6407(14)
Cs(3)-Se(11)#7	3.7102(15)	Cs(3)-Se(5)#2	3.8479(15)
Cs(3)-Se(5)	3.8810(13)	Cs(3)-Se(2)#4	3.9107(14)
Cs(3)-Se(1)	4.1392(14)	Cs(3)-Se(7)#5	4.2167(15)
Cs(3)-Se(1)#1	4.2689(15)		
Nb(1)-Se(10)#2	2.3308(13)	Nb(1)-Se(8)	2.5961(13)
Nb(1)-Se(3)#2	2.5997(12)	Nb(1)-Se(7)#1	2.6486(13)
Nb(1)-Se(5)#8	2.7003(13)	Nb(1)-Se(2)#2	2.7551(13)
Nb(1)-Se(1)#9	2.9274(13)		
Nb(2)-Se(11)	2.3217(13)	Nb(2)-Se(6)	2.5890(13)
Nb(2)-Se(9)#10	2.6159(13)	Nb(2)-Se(1)	2.6257(13)
Nb(2)-Se(4)#11	2.6312(13)	Nb(2)-Se(2)#10	2.6584(13)
Nb(2)-Se(3)#10	2.8924(12)		
As-Se(4)	2.3728(15)	As-Se(7)#5	2.3798(15)
As-Se(5)#2	2.4242(14)		
Se(1)-Se(6)	2.3738(14)	Se(2)-Se(9)	2.3567(14)
Se(3)-Se(8)#1	2.3346(13)		
For 4			
K(1)-Se(11)	3.261(3)	K(1)-Se(9)#1	3.275(3)
K(1)-Se(10)#2	3.352(3)	K(1)-As#3	3.467(3)
Nb(1)-Se(3)K(1)-Se(11)#1	3.490(3)	K(1)-Se(2)	3.635(3)
Nb(1)-Se(3)K(1)-Se(5)	3.694(3)	K(1)-Se(5)#4	3.790(3)
Nb(1)-Se(3)K(1)-Se(1)	3.915(3)		
Nb(1)-Se(3)K(2)-Se(8)	3.319(2)	K(2)-Se(11)#5	3.360(2)
Nb(1)-Se(3)K(2)-Se(9)#6	3.433(3)	K(2)-Se(6)#7	3.436(3)
Nb(1)-Se(3)K(2)-Se(3)#6	3.456(2)	K(2)-Se(11)#7	3.491(2)
Nb(1)-Se(3)K(2)-Se(1)#7	3.515(2)	K(2)-Se(10)	3.524(3)
Nb(1)-Se(3)K(2)-Se(10)#6	3.648(3)	K(2)-Se(7)	3.899(3)
Nb(1)-Se(3)K(3)-Se(4)#8	3.363(3)	K(3)-Se(4)#6	3.475(3)
Nb(1)-Se(3)K(3)-Se(10)#9	3.480(3)	K(3)-Se(8)	3.511(3)
Nb(1)-Se(3)K(3)-Se(6)	3.584(3)	K(3)-Se(3)#6	3.634(3)
Nb(1)-Se(3)K(3)-Se(5)#9	3.685(3)	K(3)-Se(1)	3.891(3)
Nb(1)-Se(3)K(3)-As#6	3.895(3)	K(3)-Se(6)#6	3.923(3)
Nb(1)-Se(3)Ta(1)-Se(10)	2.3359(9)	Ta(1)-Se(8)	2.5868(10)
Nb(1)-Se(3)Ta(1)-Se(3)	2.5992(9)	Ta(1)-Se(7)	2.6221(10)
Nb(1)-Se(3)Ta(1)-Se(5)	2.6851(10)	Ta(1)-Se(2)	2.7435(10)
Nb(1)-Se(3)Ta(1)-Se(1)	2.8920(10)		
Nb(1)-Se(3)Ta(2)-Se(11)	2.3439(10)	Ta(2)-Se(6)	2.5829(10)
Nb(1)-Se(3)Ta(2)-Se(1)	2.6145(10)	Ta(2)-Se(9)	2.6178(10)
Nb(1)-Se(3)Ta(2)-Se(4)	2.6279(10)	Ta(2)-Se(2)	2.6595(10)
Nb(1)-Se(3)Ta(2)-Se(3)	2.8315(9)		
Nb(1)-Se(3)As-Se(7)#10	2.3761(14)	As-Se(4)	2.3812(13)
Nb(1)-Se(3)	2.4242(13)		
Nb(1)-Se(3)Se(1)-Se(6)	2.3816(13)	Se(2)-Se(9)	2.3569(13)
Nb(1)-Se(3)Se(3)-Se(8)	2.3386(12)		

Table 2 (Continued)

Symmetry transformations used to generate equivalent atoms for **1**

#1 $x, -y+1, z - (1/2)$	#2 $x - (1/2), y + (1/2), z$	#3 $x + (1/2), y + (1/2), z$
#4 $x, -y+1, z + (1/2)$	#5 $x + (1/2), -y + (1/2), z - (1/2)$	#6 $x + (1/2), y - (1/2), z$
#7 $x, -y, z - (1/2)$	#8 $x, y, z - 1$	#9 $x - (1/2), -y + (1/2), z - (1/2)$
#10 $x - (1/2), -y + (1/2), z + (1/2)$		

Symmetry transformations used to generate equivalent atoms for **2**

Nb(1)-Se(3)#1 Nb(1)-Se(3) $x - (1/2), y - (1/2), z$	#2 $x, -y + 1, z - (1/2)$	#3 $x - (1/2), -y + (3/2), z - (1/2)$
Nb(1)-Se(3)#4 $x, y, z - 1$	#5 $x, -y + 2, z - (1/2)$	#6 $x, -y + 1, z + (1/2)$
Nb(1)-Se(3)#7 $x - (1/2), -y + (3/2), z + (1/2)$	#8 $x + (1/2), -y + (3/2), z + (1/2)$	#9 $x, y, z + 1$

Symmetry transformations used to generate equivalent atoms for **3**

Nb(1)-Se(3)#1 $x, -y + 2, z - (1/2)$	#2 $x, -y + 2, z + (1/2)$	#3 $x + 1, y, z$
Nb(1)-Se(3)#4 $x + (1/2), y + (1/2), z$	#5 $x + (1/2), -y + (3/2), z - (1/2)$	#6 $x+1, -y + 2, z - (1/2)$
Nb(1)-Se(3)#7 $x, y, z - 1$	#8 $x - (1/2), -y + (5/2), z + (1/2)$	#9 $x - (1/2), y + (1/2), z$
Nb(1)-Se(3)#10 $x + (1/2), -y + (3/2), z + (1/2)$	#11 $x - (1/2), -y + (3/2), z + (1/2)$	

Symmetry transformations used to generate equivalent atoms for **4**

Nb(1)-Se(3)#1 $x, -y + 1, z + (1/2)$	#2 $x + (1/2), y - (1/2), z$	#3 $x - (1/2), y - (1/2), z$
Nb(1)-Se(3)#4 $x, -y + 1, z - (1/2)$	#5 $x - (1/2), -y + (3/2), z + (1/2)$	#6 $x, -y + 2, z + (1/2)$
Nb(1)-Se(3)#7 $x - (1/2), y + (1/2), z$	#8 $x, y, z + 1$	#9 $x + (1/2), -y + (3/2), z + (1/2)$
Nb(1)-Se(3)#10 $x + (1/2), -y + (3/2), z - (1/2)$		

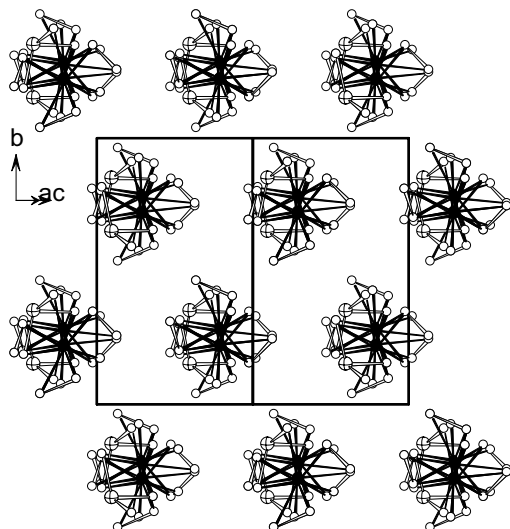


Fig. 1. Structure of **1** viewed down the [101] axis. Small black-filled circles are Nb atoms, open circles are Se atoms, and hatched circles are As atoms. Potassium cations are omitted for clarity. The polar character of the structure is clearly visible in this projection.

a common face to form a $[\text{Nb}_2\text{Se}_5(\text{Se}_2)_3]^{8-}$ dimeric core. These cores are linked along the [101] direction through a pyramidal $[\text{AsSe}_3]^{3-}$ anion to form the infinite chain $1/\infty[\text{Nb}_2\text{Se}_2(\text{Se}_2)_3(\text{AsSe}_3)]^{3-}$, Fig. 2. These chains show a noncentrosymmetric symmetry due to the arrangement of pyramidal $[\text{AsSe}_3]^{3-}$ units, Fig. 3.

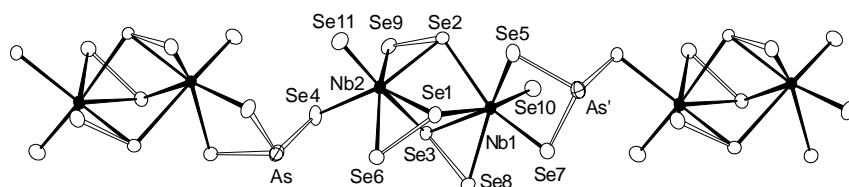


Fig. 2. The $[\text{Nb}_2\text{AsSe}_{11}]^{3-}$ chain in **1**.

The crystal structures of $\text{Rb}_3\text{Nb}_2\text{AsSe}_{11}$, **2** and $\text{Cs}_3\text{Nb}_2\text{AsSe}_{11}$, **3** contain the same structural motif as **1**, i.e., $1/\infty[\text{Nb}_2\text{Se}_2(\text{Se}_2)_3(\text{AsSe}_3)]^{3-}$ anionic chain. The average Se–Se distance is normal at 2.354, 2.354, and 2.355 Å for **1–3**, respectively, Table 2. The bond distances of Nb–Se and As–Se are normal, and the selected bond lengths of **1–3** are given in Table 2. The Nb–Nb distances within the dimeric core and between the cores are 3.694(8) and 6.108(14) Å for **1**, 3.699(3) and 6.169(5) Å for **2**, and 3.699(6) and 6.198(10) Å for **3**, which indicate no Nb–Nb bonding. The inter-chain spacings gradually increase as the size of alkali metal cations increases. The chains achieve a pseudo-hexagonal packing in which each chain is surrounded by six neighboring chains at distance of 7.646 ($\times 4$) and 8.188 Å ($\times 2$) for **1** (Fig. 1), 7.823 and 8.332 Å for **2**, and 8.090 and 8.532 Å for **3**. All three crystallographically unique K^+ cations are surrounded by 10 Se atoms in the range 3.266(3)–3.935(3) Å, 3.311(3)–3.904(3) Å, and 3.368(3)–3.945(3) Å for K(1), K(2) and K(3), respectively, Table 2. An unusually close interaction of K(1)–As and a weak interaction of K3–As are found at distance of 3.451 and 3.863 Å, respectively. Also, each of the three crystallographically independent Rb^+ and Cs^+ cations in **2** and **3** are surrounded by 10 or 11 Se atoms, Table 2. For **2** and **3**, the interactions of Rb^+ –As and Cs^+ –As occur at 3.536 and 3.625 Å, whereas the weak interactions are at distances of 3.930 and 4.081 Å, respectively. Similar interactions between the alkali metals and As atoms were

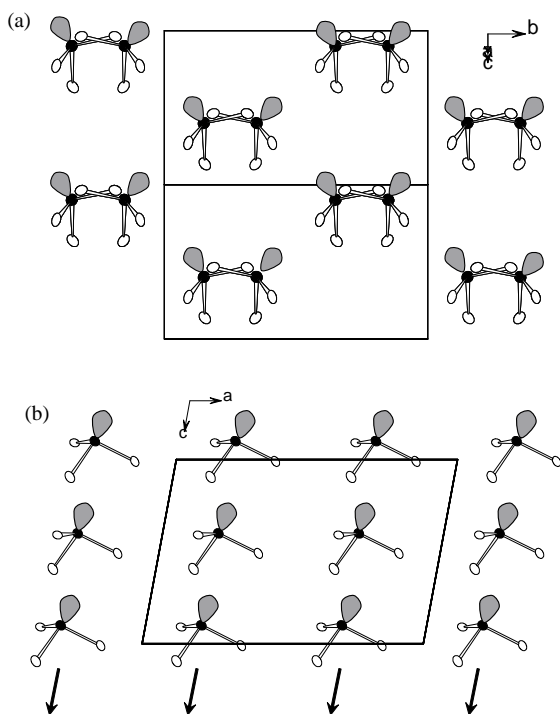
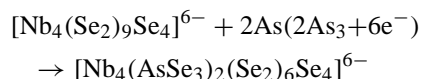
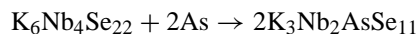


Fig. 3. $[\text{AsSe}_3]^{3-}$ moiety in the $[\text{Nb}_2\text{AsSe}_{11}]^{3-}$ chain in **1–3** along the chain direction $[101]$ (a) and along the b axis (b). The $[\text{Nb}_2\text{Se}_{11}]^{3-}$ anions in the chain were omitted to stress the noncentrosymmetric arrangement of $[\text{AsSe}_3]^{3-}$ anions. The lone pair on As^{3+} is drawn schematically. The arrows indicate the direction of the $[\text{Nb}_2\text{AsSe}_{11}]^{3-}$ chain.

also observed in $\text{K}_2\text{SnAs}_2\text{S}_6$ and $\text{Cs}_2\text{SnAs}_2\text{Q}_9$ ($\text{Q} = \text{S}, \text{Se}$) [6,7].

Several compounds containing the M_2Q_{11} unit ($\text{M} = \text{Nb}, \text{Ta}$; $\text{Q} = \text{S}, \text{Se}$) as a building block have been reported. This unit is found either as a simple dimeric core the molecule anions $[\text{Nb}_2\text{S}_{11}]^{4-}$ ($\text{M} = \text{Nb}, \text{Ta}$) in $\text{A}_4\text{Nb}_2\text{S}_{11}$ ($\text{A} = \text{K}, \text{Cs}$) [8] and $\text{A}_4\text{Ta}_2\text{S}_{11}$ ($\text{A} = \text{K}, \text{Rb}, \text{Cs}$) [9], or as in oligomeric form in which the dimeric cores are connected *via* polychalcogenide ligands, $[\text{Nb}_4\text{Q}_{22}]^{6-}$ in $\text{A}_6\text{Nb}_4\text{Q}_{22}$ ($\text{A} = \text{K}, \text{Rb}, \text{Cs}$) [8a,10] and $[\text{Nb}_4\text{S}_{25}]^{6-}$ in $\text{K}_6\text{Nb}_4\text{S}_{25}$ [11]. Also, various polyselenide ligands can bridge the dimeric cores to construct infinite polymeric chains, as in $[\text{Nb}_6\text{Se}_{35}]^{12-}$ of $\text{A}_{12}\text{Nb}_6\text{Se}_{35}$ ($\text{A} = \text{K}, \text{Rb}$) [12].

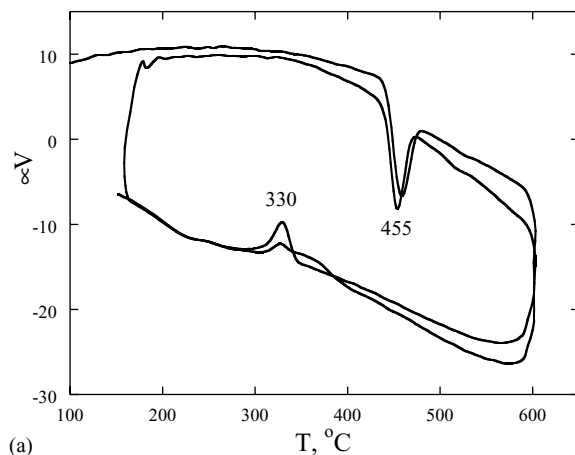
The formation of compounds **1–3** could be simply regarded as arising from the insertion reaction of As atoms into $\text{K}_6\text{Nb}_4\text{Se}_{22}$ as shown by the equations below. It is interesting that the redox center responsible for As insertion in these phases is the Se–Se bond (oxidative addition) rather than the d-block orbitals of the highly oxidized niobium/tantalum metals (d^0).



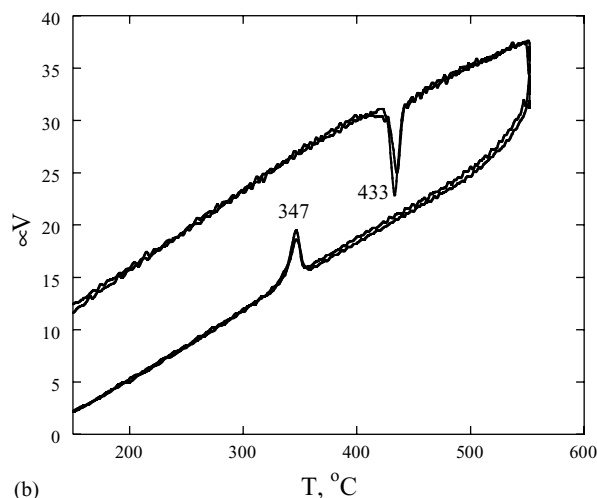
The Ta analog has similar structural characteristics and will not be discussed further. Specific structural details are given in Tables 1 and 2.

4.3. Thermal analysis

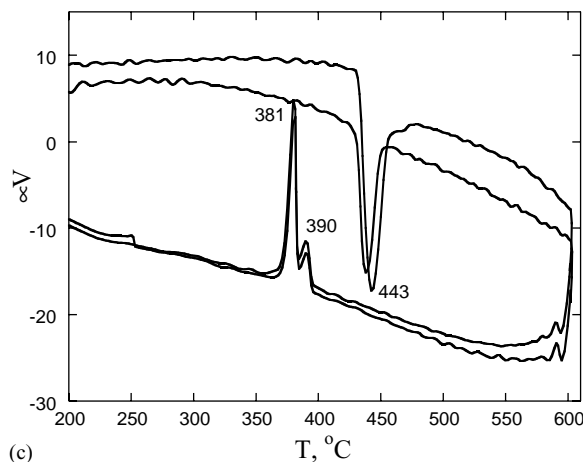
Differential thermal analysis (DTA) suggests that compounds **2**, **3** and **4** melt congruently at 455, 433 and 443,



(a)



(b)



(c)

Fig. 4. Differential thermal analysis of **2** (a), **3** (b), and **4** (c) showing melting and recrystallization temperatures.

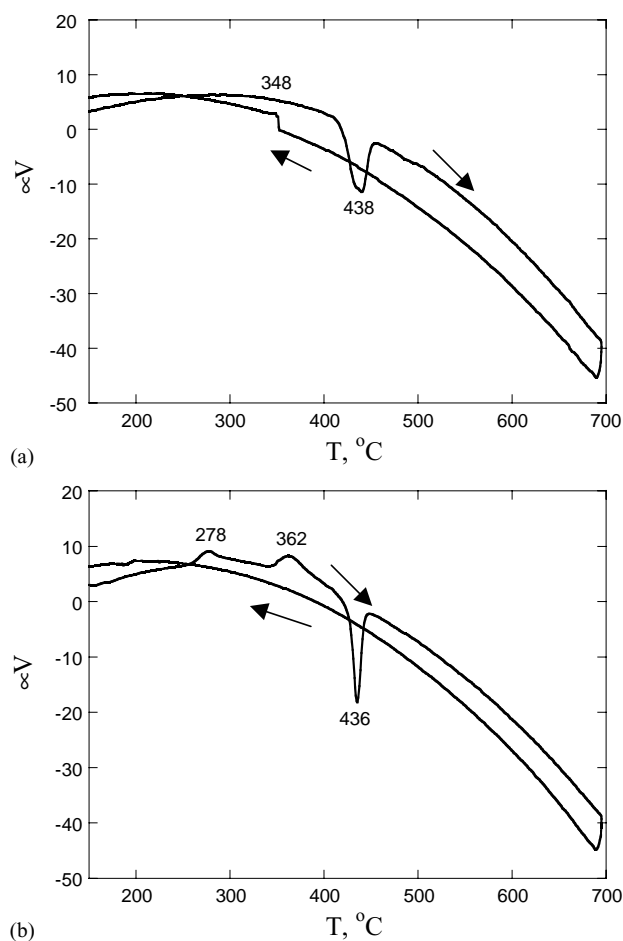


Fig. 5. Differential thermal analysis plots of **1** showing (a) melting in the first cycle with weak exothermic peak at 348°C upon cooling and (b) broad two exothermic peaks at 278 and 362°C followed by melting at 436°C in the second cycle.

respectively. For each compound, multiple heating/cooling cycles were monitored, as they exhibited well-defined melting and crystallization temperatures, Fig. 4. The powder XRD patterns of **1–4**, which are taken before and after DTA measurement, are identical, indicating no decomposition. DTA of **1** showed one endothermic peak at 438°C on heating with a small exothermic peak at 348°C on cooling, Fig. 5. The second heating/cooling cycle showed one endothermic peak at 436°C and two broad exothermic peaks at 362 and 278°C. The powder XRD patterns taken after the first and second DTA cycle suggest the products are a mixture of glass phases and unknown crystalline phases.

4.4. Spectroscopy

The solid-state diffuse reflectance UV-Vis spectra of **1–3** revealed absorption edge corresponding to band gaps of 1.53, 1.50, and 1.35 eV, respectively, Fig. 6. The heavier Ta compound **4** shows a slightly narrower optical gap than, **1** and **2**, at 1.45 eV, Fig. 6.

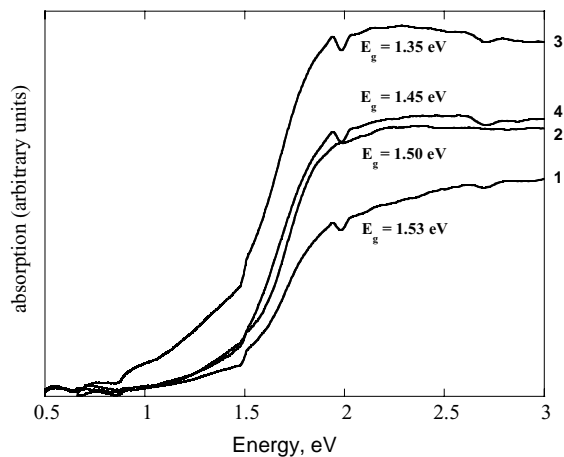


Fig. 6. Optical absorption spectra showing absorption edges at 1.53 eV for **1**, 1.50 eV for **2**, 1.35 eV for **3** and 1.45 eV for **4**.

The Raman spectra of **1–4**, display peaks at 161, 178, 186, 230, 251, 275, 292, 303, 334 cm^{-1} for **1**; 161, 178, 186, 230, 251, 275, 292, 302, 334 cm^{-1} for **2**; 164, 178, 185, 230, 251, 274, 293, 301, 334 cm^{-1} for **3**; 163, 189, 206, 234, 251, 274, 295 cm^{-1} for **4**, Fig. 7. The spectra of **1–3** containing the same $[\text{Nb}_2\text{AsSe}_{11}]^{3-}$ chain anion are similar to each other. However, in the spectrum of **4** which contains the $[\text{Ta}_2\text{AsSe}_{11}]^{3-}$ chain anion, the peaks at 178, 303 and 334 cm^{-1} in **1** are absent, instead a new peak at 206 cm^{-1} is present. Therefore, the peaks 178, 303 and 334 cm^{-1} must be associated with Nb–Se vibrational frequencies and 206 cm^{-1} with Ta–Se modes. On the basis of previous reports, the peaks ~ 230 and 251 cm^{-1} in **1–4** can be assigned to Se–Se stretching vibrations [13]. It is difficult, however, to unequivocally assign these shifts because the As–Se vibrations also occur in this region. The several weak modes at low frequencies between 161 and 189 cm^{-1} may be a result of vibrations associated with the heavy $\text{Nb}^{5+}/\text{Ta}^{5+}$ and/or alkali metal cations.

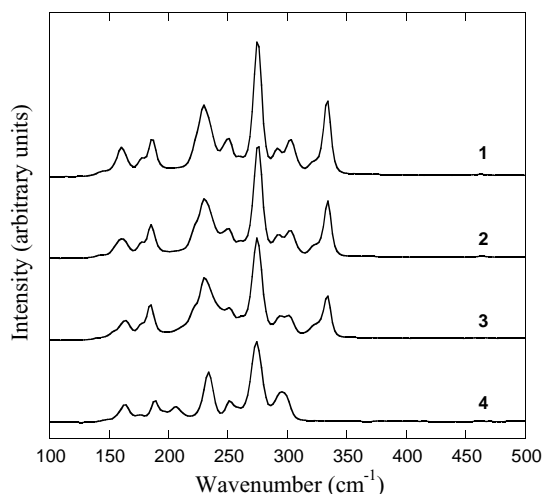


Fig. 7. Raman spectra of **1–4**.

Supporting information available: Tables of crystallographic details, atomic coordinates, isotropic and anisotropic displacement parameters for all atoms, and interatomic distances and angles for $A_3Nb_2AsSe_{11}$ ($A = K, Rb, Cs$) and $K_3Ta_2AsSe_{11}$, in CIF format. CSD-numbers $K_3Nb_2AsSe_{11}$ 413597, $Rb_3Nb_2AsSe_{11}$ 413598, $Cs_3Nb_2AsSe_{11}$ 413599, $K_3Ta_2AsSe_{11}$ 413600.

Acknowledgements

Financial support from the National Science Foundation (Grant DMR-0127644) is gratefully acknowledged.

References

- [1] R.G. Iyer, M.G. Kanatzidis, *Inorg. Chem.* 41 (2002) 3605.
- [2] R.G. Iyer, J. Do, M.G. Kanatzidis, *Inorg. Chem.* 42 (2003) 1475.
- [3] T.J. McCarthy, M.G. Kanatzidis, *J. Alloys Comp.* 236 (1996) 70–85.
- [4] SAINT, version 4.05; SADABS; SHELXTL, Version 5.03. Siemens Analytical X-ray Instruments: Madison, WI, 1995.
- [5] P. Dürichen, M. Bolte, W.J. Bensch, *Solid State Chem.* 140 (1998) 1998.
- [6] S. Schreiner, L.E. Aleandri, D. Kang, J.A. Ibers, *Inorg. Chem.* 28 (1989) 392.
- [7] Crystal data for $Cs_{21}(Nb_4Se_{22})_3(AsSe_3)$: rhombohedral, R-3; $a = 15.146(2)$, $\alpha = 91.08(2)$; $R1 = 4.33\%$, $wR2 = 14.14\%$.
- [8] (a) W. Bensch, P. Dürichen, *Eur. J. Solid State Inorg. Chem.* 33 (1996) 527;
(b) K.O. Klepp, G.Z. Gabl, *Naturforsch.* B53 (1998) 1236.
- [9] (a) S. Schreiner, L.E. Aleandri, D. Kang, J.A. Ibers, *Inorg. Chem.* 28 (1989) 392;
(b) P. Dürichen, W. Bensch, *Acta Crystallogr.* C54 (1998) 706.
- [10] (a) W. Bensch, P.Z. Dürichen, *Anorg. Allg. Chem.* 622 (1996) 1963;
(b) P. Dürichen, W.Z. Bensch, *Kristallogr.* 11 (Suppl.) (1996) 77.
- [11] W. Bensch, P. Dürichen, *Eur. J. Solid State Inorg. Chem.* 33 (1996) 1233.
- [12] P. Dürichen, M. Bolte, W. Bensch, *J. Solid State Chem.* 140 (1998) 97.
- [13] (a) K.-S. Choi, M.G. Kanatzidis, *Inorg. Chem.* 40 (2001) 101;
(b) Y. Park, M.G. Kanatzidis, *Inorg. Chem.* 40 (2001) 5913;
(c) K.-S. Choi, M.G. Kanatzidis, *Chem. Mater.* 11 (1999) 2613.